Available online at www.sciencedirect.com
ScienceDirect
European Journal of Pharmaceutics and Biopharmaceutics 70 (2008) 109–115
European Journal of Pharmaceutics and Biopharmaceutics
www.elsevier.com/locate/ejpb

Research paper

Preparation of amorphous cefuroxime axetil nanoparticles by sonoprecipitation for enhancement of bioavailability

Ravindra S. Dhumal [a], Shailesh V. Biradar [a], Shigeo Yamamura [b], Anant R. Paradkar [a,c,*], Peter York [c]

[a] Department of Pharmaceutics, Poona College of Pharmacy and Research Centre, Bharati Vidyapeeth University, Maharashtra, India
[b] Department of Pharmaceutical Sciences, Josai International University, Chiba, Japan
[c] Institute of Pharmaceutical Innovations, University of Bradford, West Yorkshire, UK

Received 19 November 2007; accepted in revised form 4 April 2008
Available online 11 April 2008

Abstract

The aim of the present work was to prepare amorphous discreet nanoparticles by sonoprecipitation method for enhancing oral bioavailability of cefuroxime axetil (CA), a poorly water-soluble drug. CA nanoparticles (SONO-CA) were prepared by sonoprecipitation and compared with particles obtained by precipitation without sonication (PPT-CA) and amorphous CA obtained by spray drying. Spray drying present broad particle size distribution (PSD) with mean particle size of 10 μm and low percent yield, whereas, precipitation without sonication resulted in large amorphous aggregates with broad PSD. During sonoprecipitation, particle size and yield improve with an increase in the amplitude of sonication and lowering the operation temperature due to instantaneous supersaturation and nucleation. The overall symmetry and purity of CA molecule was maintained as confirmed by FTIR and HPLC, respectively. All the three methods resulted in the formation of amorphous CA with only sonoprecipitation resulting in uniform sized nanoparticles. Sonoprecipitated CA nanoparticles showed enhanced dissolution rate and oral bioavailability in Wistar rat due to an increased solubility attributed to combination of effects like amorphization and nanonization with increased surface area and reduced diffusion pathway.

Keywords: Cefuroxime axetil; Sonoprecipitation; Amorphous; Nanoparticles; Bioavailability

1. Introduction

CA is 1-acetoxyethyl ester of a β-lactamase-stable cephalosporin, cefuroxime (C) with a broad spectrum of activity against Gram-positive and Gram-negative microorganisms [1]. After oral administration CA is absorbed and rapidly hydrolysed by esterases in the intestinal mucosa and portal blood to produce C. The 1-acetoxyethylester group in position 4 of CA ensures lipophilicity and promotes the intestinal absorption of C but at the same time compromise on solubility and hence, the prodrug shows poor and variable oral bioavailability [2]. CA exists in crystalline as well as amorphous form, of these latter exhibits higher bioavailability owing to improved solubility. But, its bioavailability is variable and limited to 30% in fasted and 50% in fed states [3,4]. The most successful attempt for achieving amorphous CA from commercial point of view was through spray drying [3,4].

Nanoparticles are known to improve dissolution rate and bioavailability of poorly water-soluble drugs [5–9] owing to increased surface area available for dissolution as described by the Noyes–Whitney equation [10]. Nanoparticles are generally obtained by 'top–down' process which relies on mechanical attrition [9]. However, it is energy-intensive, time-consuming and show some disadvantages in practice such as the introduction of impurities, inadequate control of particle size and electrostatic effects. In the last decade, 'bottom–up' techniques like supercritical

* Corresponding author. Department of Pharmaceutics, Bharati Vidyapeeth University, Poona College of Pharmacy and Research Centre, Erandawane, Pune 411038, Maharashtra, India. Tel.: +91 20 2543 7237; fax: +91 20 2543 9383.
E-mail address: arparadkar@rediffmail.com (A.R. Paradkar).

0939-6411/$ - see front matter © 2008 Elsevier B.V. All rights reserved.
doi:10.1016/j.ejpb.2008.04.001

fluid technology and anti-solvent precipitation have been widely investigated to obtain nanoparticles [11–13]. However, supercritical technique is expensive, difficult to control and scale-up. The amorphous CA nanoparticles obtained by controlled nanoprecipitation and high-gravity anti-solvent precipitation have also shown significantly faster dissolution as compared to micron-sized amorphous particles obtained by spray drying but exist in chain-like aggregates [13]. Poor micromixing during anti-solvent process leads to accidental zones of supersaturation and aggregation of particles. In contrast, ultrasound is proved to be a feasible mixing method to provide uniform conditions throughout the vessel during anti-solvent process.

Ultrasound intensifies the mass transfer when it propagates through a liquid medium, and initiates an important phenomenon known as cavitation. Cavitational bubbles are formed during the negative-pressure period of the sound wave. When a cavitational bubble implodes, a localized hot spot with a high temperature and pressure is formed releasing a powerful shock wave. The reason for the above phenomena is that the collapse process is very rapid. Seconds after ultrasound is applied to the mixture, the solvent and anti-solvent are mixed homogeneously. The solubility of the solute in the solvent–anti-solvent mixture is reduced sharply and immediately reaches its maximum supersaturation so that primary nucleation and crystal growth are implemented rapidly. These effects bring considerable benefits to crystallization process, such as induction of primary nucleation, reduction of crystal size, inhibition of agglomeration and manipulation of crystal size distribution [14,15]. As the number of primary nuclei increases, the amount of solute on each primary nucleus decreases, thus decreasing the size of final product. Ultrasound is also known to suppress agglomeration of product [16,17]. In our previous attempt, we have obtained sintered crystals of ibuprofen and porous amorphous particles of celecoxib with high specific surface area and dissolution properties by meltsonocrystallization [18,19].

The aim of the present study was to apply ultrasound during anti-solvent precipitation for producing discreet, non-agglomerated and amorphous CA nanoparticles for enhancement of oral bioavailability. Nanoparticles were characterized by submicron particle sizer, scanning electron microscopy (SEM), diffused reflectance infrared Fourier-transform spectroscopy (DRIFTS), differential scanning calorimetry (DSC) and X-ray powder diffraction (XRPD). In addition, improvement in the rate and extent of *in-vitro* drug dissolution from nanoparticles was justified by *in-vivo* study in Wistar rats.

2. Materials and methods

2.1. Materials

Crystalline CA with particle size 20–50 μm and indapamide were received as gift samples from Lupin Research Park (Pune, India). All other chemicals and solvents were of analytical grade.

2.2. Sonoprecipitation of CA

In this study, the equipment consisting of a probe and sonifier (Sonics and materials Inc., Vibra Cell, Model VCX 750, Connecticut, USA) was used. A probe has a tip diameter of 13 mm and is immersed 5 mm in the liquid. The device operates at a fixed wavelength of 20 kHz and is capable of inducing a maximum power output of 750 W. A 500-ml jacketed glass sonoreactor was used in these experiments providing control over temperature. Unprocessed CA was dissolved in acetone and filtered through 0.45 μm pore size membranes to remove the possible impurities. The solution was then poured into isopropyl ether kept in sonoreactor and simultaneously irradiated with varying amplitudes of ultrasonic energy for 1 min. The particles were filtered and dried under vacuum at 50 °C for 12 h and labeled as SONO-CA. Similar experiment was carried out with mechanical stirring instead of sonication to obtain PPT-CA particles.

2.3. Spray drying of CA

CA was dissolved in sufficient amount of acetone to obtain clear solution and spray dried using twin cyclone lab spray drier (LU-222 Advanced Model, Labultima, Mumbai, India), under the following set of conditions: inlet temperature 100 °C, outlet temperature, 70 °C, feed rate 4–6 ml/min, atomization air pressure 98066.5 Pa (1 kg cm^{-2}) and aspiration pressure 1961 Pa (~200 mm WC).

2.4. Thermogravimetric analysis

To determine the residual solvent in spray-dried, PPT-CA and SONO-CA, thermogravimetric analysis was performed using TA-60WS Thermogravimetric analyzer (Shimandzu, Japan). Samples (approximately 30–40 mg) were heated in platinum crucible in nitrogen atmosphere and the loss of mass as a function of temperature was recorded.

2.5. Particle size distribution

PSD of SONO-CA was determined by Nicomp 380 (PSS Corp., Santa Barbara, USA) submicron particle sizer, while PSD of spray-dried CA and PPT-CA samples was measured by Laser Diffractometer, Mastersizer 2000 Ver. 2.00 (Malvern Instruments, Malvern, UK) with obscuration not less than 10% for each measurement. The particles were dispersed in isopropyl ether and then analyzed in triplicate.

2.6. Scanning electron microscopy (SEM)

Freshly prepared PPT-CA and SONO-CA dispersions were deposited on a glass slide upon the evaporation of sol-

vent and fixed on aluminum stubs by double sided adhesive tape, while unprocessed and spray-dried CA samples were directly mounted on the aluminum stub and coated with a thin gold–palladium layer by sputter coater unit (Hitachi, E-1020, Higashi, Japan). The surface topography was analyzed with a Keyence scanning electron microscope (Keyence, V-7800, Higashi, Japan) operated at an acceleration voltage of 5 kV.

2.7. Differential scanning calorimetry (DSC)

DSC studies were carried out using Mettler-Toledo DSC 821^e instrument equipped with an intracooler (Mettler-Toledo, Switzerland). Indium and Zinc standards were used to calibrate the DSC temperature and enthalpy scale. The samples were hermetically sealed in aluminum pans and heated at a constant rate of 10 °C/min over a temperature range of 25–200 °C. Inert atmosphere was maintained by purging nitrogen gas at a flow rate of 50 ml/min.

2.8. X-ray powder diffraction (XRPD)

The XRPD patterns were recorded on X-ray diffractometer (PW 1729, Philips, The Netherlands). Samples were irradiated with monochromatized Cu-Kα radiation (1.542 Å) and analyzed from 5° to 50° 2θ. The voltage and current used were 30 kV and 30 mA, respectively. The range and the chart speed were 5×10^3 CPS and 10 mm/° 2θ, respectively.

2.9. Diffuse reflectance infrared Fourier-transform spectroscopy (DRIFTS)

The DRIFTS spectra were obtained, after appropriate background subtraction using an FTIR spectrometer (FT/IR-4100, Jasco, Japan). Samples were mixed with dry potassium bromide and scanned from 4000 to 400 cm^{-1}. Jasco spectra manager Ver. 2 was used for data acquisition and analysis.

2.10. In-vitro drug release

The dissolution studies were performed using USP 24 type II dissolution test apparatus (TDT-06P, Electrolab, India). Samples were placed in a dissolution vessel containing 900 ml 0.1 N HCl, maintained at 37 ± 0.5 °C and stirred at 100 rpm. Samples were collected periodically and replaced with a fresh dissolution medium. After centrifugation and filtration through 0.45 μm filter paper, concentration of CA was determined spectrophotometrically at 278 nm after suitable dilution. Data were analyzed by PCP-Disso software (V3, Poona College of Pharmacy, Pune, India).

2.11. Bioavailability study

Rat has been reported as a suitable model for assessing the intestinal absorption of drugs in humans [20]. Thus rat as an experimental animal was selected for the present study. All studies were approved by the Institutional Animal Ethics Committee of Poona College of Pharmacy (Pune, India), and were conducted under the provisions of the approved protocol.

2.11.1. Experimental procedure

Bioavailability (BA) of SONO-CA and PPT-CA was determined in comparison with unprocessed and spray-dried CA in healthy Wistar rats of either sex, each weighing between 200 and 250 g. Animals were fasted overnight prior to dosing. Water was allowed *ad libitum.* The animals were randomly divided into three groups of six animals each. BA was assessed after single oral dosing of sample (50 mg/kg) in the aqueous suspension form (prepared in 0.25% w/v carboxymethyl cellulose just before dosing). After mild anesthetization of animals, serial blood samples (0.5–1 ml each) were collected using retro orbital puncture technique, at predetermined time intervals (0, 15, 30, 45, 60, 90, 180, 240, 300, 1200 and 1440 min). Plasma was separated by centrifugation at 3000 rpm, 4 °C, 15 min (Cryocentrifuge 2810R, Eppendorf, USA) and promptly analyzed by HPLC.

2.11.2. Assay of plasma concentration

Plasma (200 μl) was transferred to stoppered test tube, to which 200 μl of internal standard (Indapamide, stock solution 10 μg/ml in mobile phase) was added. The sample was mixed by vortexing for 5 min. Deproteinizaton and extraction of CA and internal standard was carried out using 600 μl of acetonitrile with vortex mixing for 5 min. The solution was filtered through 0.45 μm membrane filter and analyzed by a HPLC method.

The HPLC system specifications were as follows: pump, PU-1580 (JASCO, Japan); injector, auto sampler (AS-1555; JASCO); column, RP C_{18}, 250×4.6 mm, 5 μ (Thermo Electron Corporation, USA); detector, UV/Visible (UV-1575; JASCO). Data acquisition and analysis were carried out using Borwin/HSS 2000 software (LG 1580-04; JASCO). The chromatographic conditions were as follows: mobile phase 0.01 M potassium dihydrogen phosphate and methanol (60:40, pH 5); flow rate, 1.5 ml/min; wavelength, 278 nm. The calibration curves of CA covered a concentration range of 0–25 μg/ml. The ratio of peak area of CA/Indapamide was used for quantification of plasma samples.

3. Results and discussion

3.1. Particle size and morphology

Preliminary sonoprecipitation experiments with acetone as a solvent and isopropyl ether as an anti-solvent were carried out by varying sonication amplitude, sonication time and processing temperature. Processing at lower temperature resulted in early precipitation with smaller particles and improved product yield. Therefore, all the experiments were carried out at ~5 °C. The sonication was stopped

after 1 min when complete precipitation was observed visually and confirmed from the particle size and yield. At shorter period of sonication (<1 min), rapid precipitation occurred followed by agglomeration. However, sonication for 1 min was enough to reduce particle growth and agglomeration. The complete liberation of supersaturation occurred in 1 min and hence, further increase in the sonication time did not show any alteration in particle size and PSD. The mean particle size of SONO-CA processed at 5 °C for 1 min was 130 nm at 25% sonication amplitude and 80 nm at 50% sonication amplitude (Fig. 1). The uniformity and spherical nature of discreet nanoparticles without agglomeration was observed in the photomicrograph of SONO-CA (Fig. 3D). The process yield of SONO-CA particles was in the range of 95.02–98.56% w/w. PPT-CA was processed by anti-solvent process without sonication as a control experiment. PPT-CA showed very large particles with broad PSD ranging from 10 to 100 μm (Fig. 2)

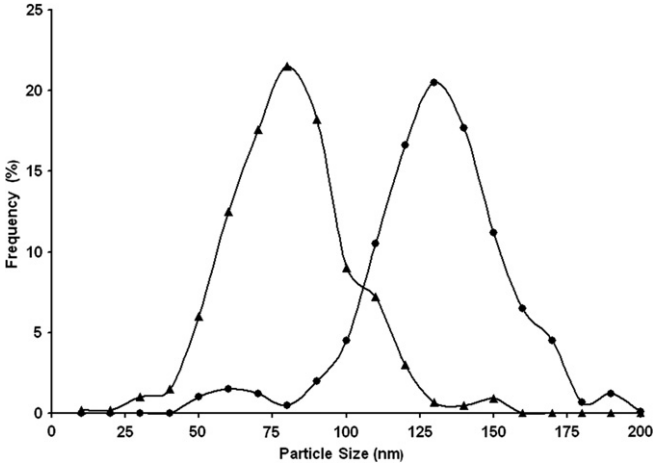

Fig. 1. Particle size distribution of SONO-CA particles obtained at 25% (●) and 50% (▲) sonication amplitude.

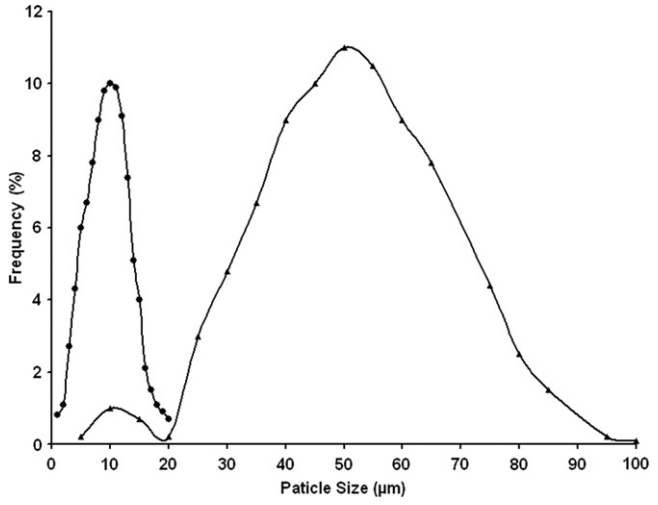

Fig. 2. Particle size distribution of spray dried CA (●) and PPT-CA (▲) particles.

and product yield of 60.20–66.07%. The aggregation of fine particles into large micron-sized porous aggregates was confirmed from the photomicrographs of PPT-CA (Fig. 3C).

When drug solution is added into the anti-solvent, it does not disperse immediately and produces local zones of excessive supersaturation. When anti-solvent process uses mechanical stirring, poor micromixing is unavoidable, which increases the precipitation rate locally leading to agglomeration and increase in particle size as observed in PPT-CA. In contrast homogeneous micromixing during ultrasonication maintains reasonably uniform conditions throughout the vessel causing the formation of nanosized discreet SONO-CA particles.

Since spray drying is the current benchmark technique for generation of amorphous CA microparticles [3,4], the SONO-CA particles were also compared with amorphous CA obtained by spray drying. Spray drying process variables were optimized on the basis of production yield and powder characteristics. Production yield for spray-dried CA was 55.72% w/w. The particle size of spray-dried CA was reduced compared with the unprocessed CA with mean particle size of 10 μm. However, the PSD was broad (Fig. 2). The Fig. 3B shows spherical smooth CA particles obtained by spray drying, compared to unprocessed CA which showed irregular shaped crystalline particles with size in the range of 20–50 μm (Fig. 3A). The effect of ultrasonic energy and spray drying process on the chemical stability of the product was examined by DRIFTS and HPLC. DRIFT spectra and chromatograms of spray dried CA, PPT-CA and SONO-CA were similar to unprocessed CA, indicating the absence of chemical degradation during processing. The amount of residual organic solvent in the samples was below the detection limit of TGA (<0.05% w/w).

3.2. DSC and XRPD

The DSC scan of unprocessed CA showed a single endotherm at 181 °C ascribed to melting of drug (Fig. 4). However, spray dried CA, PPT-CA and SONO-CA did not show melting endotherm at 181 °C and exhibited small endothermic change in the heat capacity at 91–94 °C, earlier reported as the T_g [21]. It proved that the spray dried, PPT-CA and SONO-CA were in amorphous form. In order to further confirm the physical state, XRPD studies were performed. The XRPD patterns of unprocessed CA showed characteristic high-intensity diffraction peaks at 2θ values of 5.60°, 7.84°, 9.07°, 11.92°, 15.81°, 19.23°, 22.64° and 24.95°, indicating crystalline nature of unprocessed CA (Fig. 5). However, instead of intense crystalline peaks spray dried CA produced a halo pattern typical of an amorphous material, where the broad and diffused maxima are caused by a random arrangement of the constituent molecules. The diffractograms of PPT-CA and SONO-CA also showed similar halo and diffused pattern confirming the conversion of CA into amorphous from during

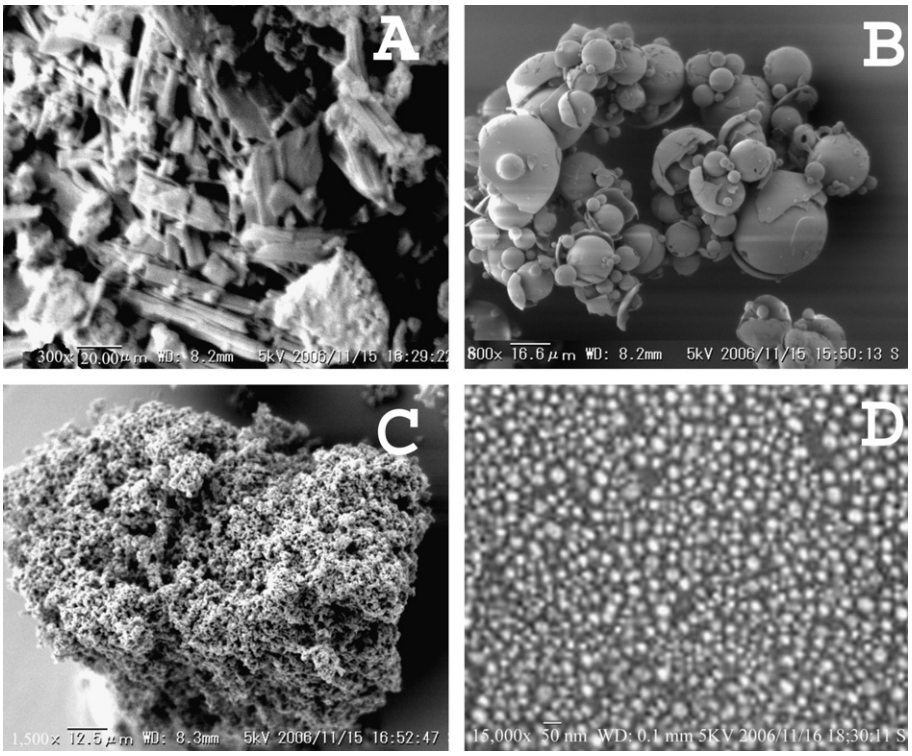

Fig. 3. SEM photomicrographs of (A) unprocessed CA, (B) spray-dried CA, (C) PPT-CA and (D) SONO-CA.

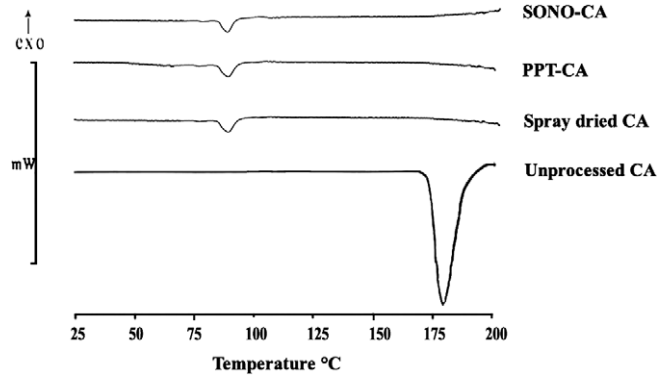

Fig. 4. DSC curves of unprocessed CA, spray-dried CA, PPT-CA and SONO-CA.

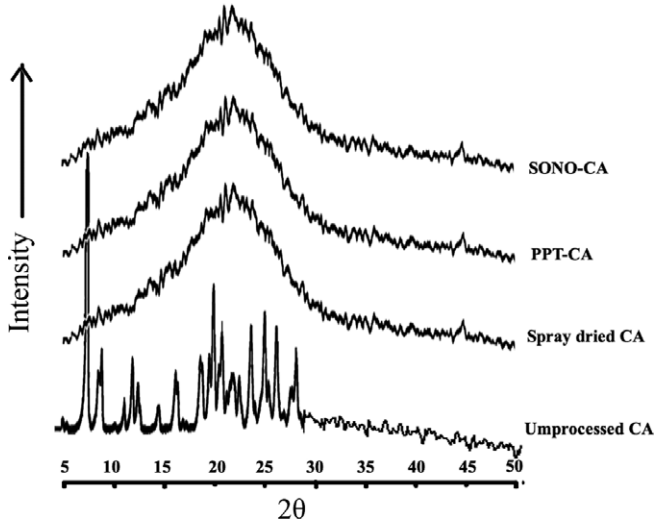

Fig. 5. XRPD patterns of unprocessed CA, spray-dried CA, PPT-CA and SONO-CA.

spray drying, precipitation with sonication and without sonication.

3.3. Dissolution

The dissolution profiles of unprocessed and processed CA are shown in Fig. 6. The unprocessed CA did not achieve complete dissolution during the 150-min testing period and only 45% drug was released at the end of 150 min, owing to its crystalline nature and larger crystal size. Spray-dried CA showed some enhancement in dissolution with 70% of drug released during 150 min testing period. This increase in dissolution was attributed to amorphization of CA. PPT-CA showed 59% drug release in 30 min and 79% drug release at the end of 150 min. This enhancement in dissolution can be partly attributed to amorphization as in spray drying. But, the further increase in the dissolution of PPT-CA is due to the porous nature of the aggregates, which are made up of fine subunits that are hold together in the form of aggregate (as seen in Fig. 3C), increasing the effective surface area available for dissolution. However, 91% of SONO-CA was dissolved in 30 min and complete dissolution occurred within 60 min. This was attributed to the combination of effects like amor-

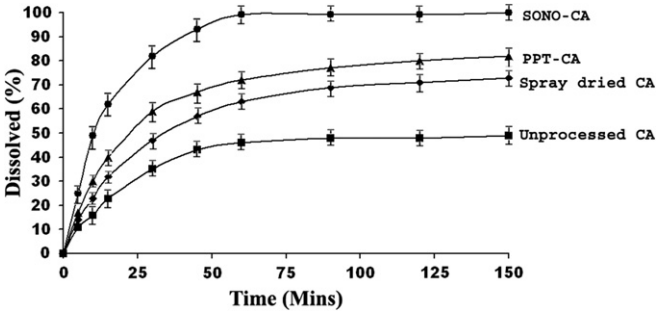

Fig. 6. Dissolution profiles of unprocessed CA, spray-dried CA, PPT-CA and SONO-CA.

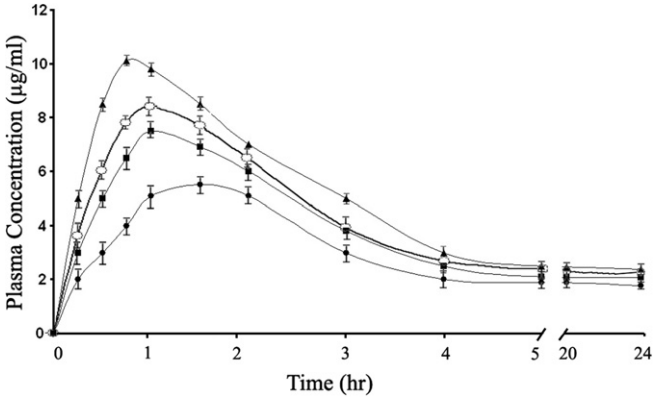

Fig. 7. Representative plasma concentration *vs* time profiles after oral administration of unprocessed CA (●), spray dried CA (■), PPT-CA (O) and SONO-CA (▲) in rat.

phization and particle size which was reduced to nano scale without aggregation (as seen from Fig. 3D), greatly increasing the specific surface area and decreasing diffusion layer thickness. These promising results in *in-vitro* drug release studies promoted us to perform *in-vivo* studies in rat.

3.4. Bioavailability study

The *in-vivo* study in Wistar rats was performed to quantify C, after administering formulations of CA orally in suspension form. The HPLC method and extraction process were well validated. The ratio of CA to indapamide (internal standard) concentration was linear. The plasma profiles of C in adult Wistar rats following oral administration of the unprocessed, spray dried, PPT-CA and SONO-CA were compared. A summary of pharmacokinetic parameters and plasma concentration *vs* time curves is shown in Table 1 and Fig. 7, respectively. The plasma concentration profile of C for SONO-CA represents significant improvement in drug absorption than the spray dried PPT-CA or unprocessed CA. Both the C_{max} and AUC_{0-24h} values of SONO-CA were approximately one-half fold greater than those of the spray-dried CA and two fold greater than crystalline CA, indicating a remarkable improvement in the oral absorption of CA when administered in the form of amorphous nanoparticles. PPT-CA also showed improvement in C_{max} and T_{max} over unprocessed and spray-dried CA owing to amorphous and porous nature of particles. This was in agreement with the *in-vitro* dissolution studies. SONO-CA was found to exhibit better bioavailability as compared to unprocessed (crystalline), spray dried and PPT-CA because of its greater dissolution rate owing to its amorphization and reduced particle size with increased surface area and reduced diffusion layer thickness. Moreover, immediate release of drug also makes it available at the site of absorption avoiding its passage to the distal segments where it may be hydrolyzed into non-absorbable C.

4. Conclusions

Application of ultrasound during anti-solvent precipitation caused intensified micromixing leading to enhanced mass transfer between solvent and anti-solvent, inducing instantaneous high levels of supersaturation to produce amorphous CA nanoparticles with narrow PSD. These nanoparticles showed dramatic improvement in rate as well as extent of *in-vitro* drug release and oral bioavailability in Wistar rat. This is attributed to amorphization, increased surface area and decreased diffusion layer thickness. This study demonstrates potential of sonoprecipitation technique to obtain discreet and amorphous nanoparticles with feasibility for scale-up.

Acknowledgements

Anant R. Paradkar is thankful to British Council for UK–India Education and Research Initiative (UKERI) Fellowship, Bharati Vidyapeeth University, Pune, India, for the sabbatical leave and AICTE (New Delhi, India) for grant in the form of Research Promotion Scheme. Ravindra S. Dhumal and Shailesh V. Biradar are thankful to CSIR (New Delhi, India) for providing financial support in the form of senior research fellowship. The authors are thankful to the Faculty of Pharmaceutical Sciences, Toho University, Japan for providing SEM facilities and Prof. Norio Sahashi for carrying out SEM analysis and

Table 1
Pharmacokinetic parameters of unprocessed, spray-dried, PPT-CA and SONO-CA after oral dose in Wistar rat

Pharmacokinetic parameter	Unprocessed CA	Spray dried CA	PPT-CA	SONO-CA
C_{max} (μg/ml)	5.5 ± 1.03	7.1 ± 1.13	7.8 ± 1.21	10.1 ± 1.56
$T_{max\ (Min)}$	90	60	60	45
AUC_{0-24h} (μg h/ml)	65 ± 1.56	81 ± 2.21	91 ± 3.25	125 ± 1.25

Means ± SD, $n = 6$.

Dr. P. K. Khanna, Nanoscience group, Centre for Materials for Electronic Materials (C-MET), Pune, India for providing facilities at C-MET. The authors acknowledge Lupin Research Park (Pune, India) for providing gift samples of CA.

References

[1] G.K. McEvoy, Cephalosporins: cefuroxime sodium. Cefuroxime axetil, in: AHFS Drug Information, American society for Hospital Pharmacists Inc., Bethesda, MD, 2003, pp. 223–231.
[2] A. Finn, A. Straugun, M. Meyer, J. Chubb, Effect of dose and food on the bioavailability of cefuroxime axetil, Biopharm. Drug Dipos. 8 (1987) 519–526.
[3] H.A. Crisp, J.C. Clayton, Amorphous form of cefuroxime ester, U.S. Patent 4,562,181, 1985.
[4] H.A. Crisp, J.C. Clayton, L.G. Elliott, E.M. Wilson, Preparation of a Highly pure substantially amorphous form of cefuroxime axetil, U.S. Patent 4,820,1833, 1989.
[5] R.H. Muller, A. Akkar, Drug nanocrystals of poorly soluble drugs, in: J.A. Schwarz, C. Contescu, K. Putyera, (Eds.), Encyclopedia of Nanoscience and Nanotechnology. Marcel Dekker, New York, pp. 627–638.
[6] V.B. Patravale, A.A. Date, R.M. Kulkarni, Nanosuspensions: a promising drug delivery strategy, J. Pharm. Pharmacol. 56 (2004) 827–840.
[7] Y. Wu, A. Loper, E. Landis, L. Hettrick, L. Novak, K. Lynn, C. Chen, K. Thompson, R. Higgins, U. Batra, S. Shelukar, G. Kwei, D. Storey, The role of biopharmaceutics in the development of a clinical nanoparticle formulation of MK-0869: a beagle dog model predicts improved bioavailability and diminished food effect on absorption in human, Int. J. Pharm. 285 (2004) 135–146.
[8] M. Mosharraf, C. Nystrom, The effect of particle size and shape on the surface specific dissolution rate of micronized practically insoluble drugs, Int. J. Pharm. 122 (1995) 35–47.
[9] F. Kesisoglou, S. Panmai, Y. Wu, Nanosizing – oral formulation development and biopharmaceutical evaluation, Adv. Drug Deliv. Rev. 5916 (2007) 31–44.
[10] A. Noyes, W. Whitney, The rate of solution of solid substances in their own solutions, J. Am. Chem. Soc. 19 (1897) 930–934.
[11] P. Pathak, G.L. Prasad, M.J. Meziani, A.A. Joudeh, Y.P. Sun, Nanosized paclitaxel particles from supercritical carbon dioxide processing and their biological evaluation, Langmuir 23 (2007) 2674–2679.
[12] J. Zhang, Z. Shen, J. Zhong, T. Hu, J. Chen, Z. Ma, J. Yun, Preparation of amorphous cefuroxime axetil nanoparticles by controlled nanoprecipitation method without surfactants, Int. J. Pharm. 323 (2006) 153–160.
[13] J.F. Chen, J.Y. Zhang, Z.G. Shen, J. Zhong, J. Yun, Preparation and characterisation of amorphous cefuroxime axetil drug nanoparticles with novel technology: high-gravity antisolvent precipitation, Ind. Eng. Chem. Res. 45 (2006) 8723–8727.
[14] M.D. Luque de Castro, F. Priego-Capote, Ultrasound-assisted crystallization (sonocrystallization), Ultrason. Sonochem. 14 (2007) 717–724.
[15] M. Louhi-Kultanen, M. Karjalainen, J. Rantanen, M. Huhtanen, J. Kallas, Crystallization of glycine with ultrasound, Int. J. Pharm. 320 (2006) 23–29.
[16] Z. Guo, M. Zhang, H. Li, E. Wang, E. Kougoulos, Effect of ultrasound on anti-solvent crystallization process, J. Cryst. Growth 273 (2005) 555–563.
[17] H. Li, J. Wang, Y. Bao, Z. Guo, M. Zhang, Rapid sonocrystallization in the salting-out process, J. Cryst. Growth 247 (2003) 192–198.
[18] M. Maheshwari, H. Jahagirdar, A.R. Paradkar, Melt sonocrystallization of ibuprofen: effect on crystal properties, Eur. J. Pharm. Sci. 25 (2005) 41–48.
[19] A.R. Paradkar, M. Maheshwari, R.N. Kamble, I. Grimsey, P. York, Design and evaluation of celecoxib porous particles using melt sonocrystallization, Pharm. Res. 23 (2005) 1395–1400.
[20] Y.H. Zhao, M.H. Abraham, J. Le, A. Hersey, C.N. Luscombe, G. Beck, B. Sherborne, I. Cooper, Evaluation of intestinal absorption data and correlation with human intestinal absorption, Eur. J. Med. Chem. 38 (2003) 233–243.
[21] S.W. Jun, M.S. Kim, G.H. Jo, S. Lee, J.S. Woo, J.S. Park, S.J. Hwang, Cefuroxime axetil solid dispersions prepared using solution enhanced dispersion by supercritical fluids, J. Pharm. Pharmacol. 57 (2005) 1529–1537.